International Journal of Heat and Technology
Vol. 43, No. 4, August, 2025, pp. 1439-1448
Journal homepage: http://iieta.org/journals/ijht

Intelligent Smoke Control of Supply-Exhaust Air Curtains in Highway Tunnels under Dual Fire Source Conditions

Shoupu Lu[1], Yang Xu[2*], Xiaoyan Li[2], Mengnan Kou[2]

[1] School of International Education, Henan University of Economics and Law, Zhengzhou 450002, China
[2] School of Smart Energy and Environment, Zhongyuan University of Technology, Zhengzhou 450007, China

Corresponding Author Email: 20100132@huel.edu.cn

https://doi.org/10.18280/ijht.430421

Received: 18 January 2025
Revised: 19 June 2025
Accepted: 10 July 2025
Available online: 31 August 2025

Keywords:
supply-exhaust air curtains, FDS, dual fire source heat release rates, smoke exhaust efficiency

ABSTRACT

The rapid development of highway tunnels has increased the potential risk posed by dual fire source incidents, where smoke propagates rapidly and temperatures rise sharply, severely threatening human safety. The supply-exhaust air curtain has emerged as an efficient smoke prevention and exhaust technology; however, its performance under dual fire source conditions remains insufficiently investigated. In this study, a highway tunnel model was established using the Fire Dynamics Simulator (FDS) to examine the effects of varying dual fire source heat release rates (5 MW, 10 MW, and 20 MW) and air curtain operating parameters—specifically supply velocities of 2–6 m/s and exhaust velocities of 3–14 m/s—on smoke control, temperature distribution, visibility, carbon monoxide (CO) concentration, and smoke exhaust efficiency. The results indicate that a supply velocity of 2 m/s combined with an exhaust velocity of 4–8 m/s effectively inhibited smoke spread, while maintaining temperatures below 60°C, visibility above 10 m, and CO concentrations below 50 ppm at a height of 1.8 m, thereby satisfying safe evacuation criteria. Higher fire source heat release rates necessitated increased exhaust velocities; however, excessively high exhaust velocities induced entrainment effects that promoted smoke descent. For all tested dual fire source scenarios, exhaust velocities of 8 m/s yielded smoke exhaust efficiencies exceeding 50%. These findings provide theoretical support for parameter design of supply-exhaust air curtains and enhance smoke prevention and exhaust strategies in highway tunnels under dual fire source fire conditions.

1. INTRODUCTION

In recent years, the rapid increase in highway tunnel construction in China has been driven by the mountainous and geologically complex terrain of many regions, the widespread utilization of underground space due to accelerated urbanization, and other factors. With the rapid development of the social economy and strong support from national policies, the scale of highway tunnels in various regions of China has continued to expand. By the end of 2023, the total highway mileage in China had reached 5.4368 million kilometers, representing an increase of 82,000 kilometers compared with the end of 2022 [1]. Although the construction and use of highway tunnels shorten travel distances, alleviate traffic congestion, and promote economic development [2], the narrow and elongated spatial structure of tunnels poses severe safety challenges during fire incidents. In the event of a fire, high-temperature smoke rapidly accumulates and spreads beneath the tunnel ceiling under buoyancy forces, significantly affecting structural integrity and safe evacuation [3]. Dual fire source incidents represent a critical escalation pathway from single-source fires to multi-source or large-scale tunnel fires [4]. The high-temperature smoke generated by the fire source is the primary lethal factor in tunnel fire accidents [5]. As a flexible barrier, an air curtain can effectively block smoke propagation without impeding normal pedestrian movement [6]. The form of supply-exhaust air curtain examined in this study employs downward supply and upward exhaust, and its smoke prevention and exhaust performance under severe dual fire source conditions was investigated to provide enhanced safety protection in tunnel fires. The design optimization of supply-exhaust air curtains for dual fire source smoke control in highway tunnels therefore holds considerable research significance.

Extensive research has been conducted by scholars both domestically and internationally on the smoke control and exhaust performance of air curtains in tunnel fire scenarios. Krajewski and Węgrzyński [7] conducted a comparative study using both numerical simulations and experimental methods to investigate the influence of jet angle and velocity on the performance of air curtains. The study also validated the feasibility of applying a single-sided smoke-control air curtain in long corridor-type buildings. Jung et al. [8] employed computational fluid dynamics (CFD) simulations to examine different jet angles and velocities of smoke-blocking air curtains in tunnel environments. The results indicate that an air curtain with a 0° jet angle fails to effectively prevent the dispersion of fire-induced smoke in tunnels. The incoming

smoke flow initially disrupts the air curtain's integrity near the tunnel sidewalls. In contrast, an optimal smoke-blocking efficiency was achieved when the air curtain was oriented at a 20° jet angle. Ji et al. [9] validated the smoke-blocking performance of a push-pull air curtain through small-scale experiments, showing that its performance exceeded that of sidewall exhaust systems and that, compared with a single-jet air curtain, it did not interfere with normal evacuation. Their analysis indicated that the greater the supply air velocity, the better the smoke control effect, and that the influence of jet velocity was greater than that of the curtain's cross-sectional area. Gao et al. [10] conducted full-scale tests to examine the smoke containment performance of air curtains in tunnel fires, reporting that supply velocities of 12 m/s and 16 m/s could respectively block smoke propagation from 1 MW and 2 MW fires. Moureh and Yataghene [11] used FDS to study smoke spread patterns under varying exhaust port spacing and air curtain spacing, finding that an exhaust port spacing of 60 m and an air curtain spacing of 120 m produced the most favorable smoke temperature and related parameters for safe evacuation.

Halawa [12] demonstrated that, compared with straight air curtains, L-shaped air curtains can significantly improve visibility, reduce smoke temperature and concentration, and enhance smoke exhaust performance through favorable interactions with ventilation and exhaust openings. Zhang and Han [13] proposed a combined approach involving an external air supply platform curtain and mechanical smoke exhaust, investigating the influence of different jet velocities at a 20° curtain angle on smoke propagation. It was found that the enhancement of fire combustion by the air curtain outweighed the cooling effect of the make-up air. Lu et al. [14] conducted 1:10 scale model experiments to examine the effects of heat release rate, jet velocity, longitudinal airflow velocity, and bifurcation angle on the smoke-sealing efficiency of air curtains, and developed a predictive model for the optimal jet velocity in bifurcated tunnels. Yu et al. [15] performed small-scale experiments to assess the smoke containment performance of air curtains in tunnel fires, identifying key performance parameters based on velocity, width, and angle. The study also revealed that when a fire occurs on one side of an air curtain, the optimal injection angle should be 30° relative to the fire source. Zhang et al. [16] constructed a physical tunnel model to investigate the temporal variations of CO concentration, visibility, and temperature under different jet velocities, and determined that a jet velocity of 14 m/s provided the most effective smoke control. As a highly effective smoke prevention and exhaust device for tunnel fires, air curtain research can be categorized into three main directions: coupling with other smoke exhaust systems, developing new air curtain configurations, and optimizing parameters such as velocity and angle.

Extensive investigations have also been conducted on dual fire source scenarios, focusing on combustion characteristics, heat release rates, flame behavior, maximum ceiling temperatures, and temperature distributions in tunnels. He et al. [17] conducted reduced-scale tunnel fire experiments to study dual fire sources of varying sizes and spacings, revealing the attenuation pattern of ceiling smoke temperatures and the influence of adjacent fire sources on temperature changes. Guo et al. [18] conducted four full-scale fire experiments to investigate the characteristics of dual fire sources. By analyzing parameters such as heat release rate, vertical temperature distribution, and flame deflection angle, it was determined that variations in the spacing between fire sources and in the ventilation rate can alter the coupling state of the thermal feedback mechanism as well as the entrainment effect between the two fire sources. Case analyses have indicated that vehicle collisions, flame deflection under longitudinal ventilation, and the spread of high-temperature smoke can easily trigger dual fire source incidents in tunnels. Fires can escalate from an initial single-source event to a dual-source scenario, markedly increasing both scale and hazard [19-21]. The smoke spread and temperature distribution of dual fire source incidents are more complex than those of single fire source cases, posing greater challenges to evacuation safety. To date, limited research has addressed the performance of air curtains in dual fire source tunnel fires. By optimizing the operating parameters of supply-exhaust air curtains, smoke containment efficiency can be improved, energy consumption reduced, and safe evacuation ensured. Therefore, in this study, FDS was employed to investigate the smoke prevention and exhaust performance of supply-exhaust air curtains in highway tunnels under dual fire source conditions, thereby providing technical support for parameter selection in their design.

2. NUMERICAL SIMULATION AND COMPUTATIONAL PARAMETERS

2.1 Model development

As shown in Figure 1, a supply-exhaust air curtain highway tunnel model was established using FDS. The tunnel model was configured with dimensions of 120 m (length) × 10 m (width) × 5 m (height), representing a central section of the Qinling Zhongnanshan Highway Tunnel. In accordance with the Code for Fire Protection Design of Buildings (GB 50016), which specifies the use of sectional ventilation in extra-long tunnels, a 120 m tunnel segment was selected for the sectional fire simulation. The initial ambient temperature in the tunnel was set to 20℃, and the atmospheric pressure was fixed at the standard value of 101.325 kPa. All four tunnel walls were assigned the material property concrete with a thickness of 0.1 m. Under natural ventilation conditions, both tunnel portals were defined as open boundaries to simulate a connection with the external environment, representing normal traffic operation.

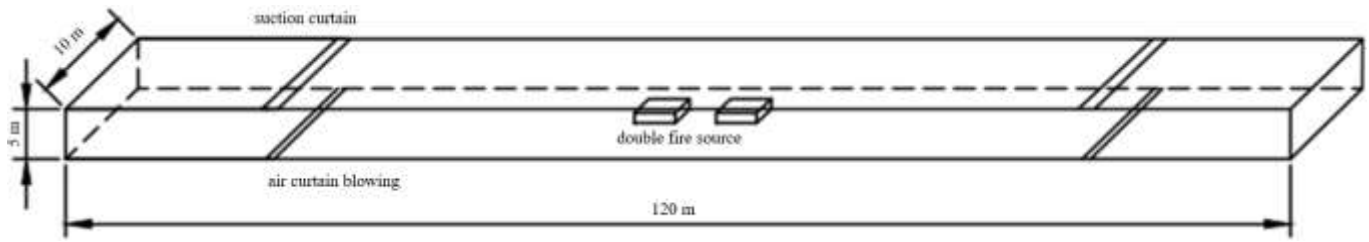

Figure 1. Highway tunnel model

In accordance with the NFPA 502, the heat release rates for passenger cars, trucks, and buses were set to 5 MW, 10 MW, and 20 MW, respectively [22]. The fire source dimensions were defined as 4 m × 2 m × 1 m for the 5 MW and 10 MW cases, and 6 m × 2 m × 2 m for the 20 MW case. The tops of both fire sources were designated as burners, with n-heptane selected as the fuel for each. Steady-state ultra-fast fire conditions were applied. Fire sources A and B were positioned symmetrically on either side of the tunnel's central axis, with a separation distance of 4 m between their centers. The supply-exhaust air curtain system was arranged with the supply curtain installed at the shallow-buried bottom of the tunnel (without obstructing traffic flow) and the exhaust curtain installed at the top. In accordance with the findings of relevant studies on supply-exhaust air curtains [23], the spacing between the two ends of the air curtain system was set to 80 m. The supply curtain was configured as supply, while the exhaust curtain was configured as exhaust. In practical applications, the supply-exhaust air curtain system does not require the installation of dedicated smoke exhaust ducts; however, supply fans and return fans are typically employed.

2.2 Measurement point arrangement and operating condition settings

To obtain the simulation data, measurement points were arranged as follows: smoke temperature and CO concentration sensors were placed 4.9 m above the tunnel centerline, with one measurement point installed every 1 m along the tunnel, resulting in a total of 120 points. Visibility sensors were positioned at a height of 1.8 m to represent human eye level, while CO volumetric flow rate sensors were located beneath the exhaust curtain. In addition, temperature and velocity slices were positioned along the Y-axis to visualize the overall and local smoke propagation and flow patterns.

Table 1. Simulation operating conditions

Case No.	Fire Source A	Fire Source B	Supply Velocity	Exhaust Velocity	Supply Curtain Width	Exhaust Curtain Width
1-6	5 WM	5 WM	2 m/s	1 m/s, 3 m/s, 4 m/s, 8 m/s, 12 m/s, and 14 m/s	0.8 m	1.6 m
7-11	10 WM	10 WM	2 m/s	3 m/s, 4 m/s, 8 m/s, 12 m/s, and 14 m/s		
12-16	20 WM	20 WM	2 m/s	3 m/s, 4 m/s, 8 m/s, 12 m/s, and 14 m/s		
17-19	20 WM	20 WM	4 m/s, 6 m/s, and 8 m/s	8 m/s		

The simulations were conducted by varying the dual fire source heat release rates and the supply and exhaust velocities of the air curtain. The effects on key evacuation safety parameters—namely smoke temperature, CO concentration, and visibility within the evacuation zone—were analyzed. The operating conditions are presented in Table 1. In accordance with relevant safety standards for emergency evacuation [24], the following criteria were applied: (a) the smoke temperature at 1.8 m above the floor should remain below 60℃; (b) visibility should exceed 10 m; and (c) the CO molar fraction should not exceed 250 × 10^{-6} mol/mol.

2.3 Grid division

Before conducting simulations in FDS, a grid independence verification must be performed, as grid resolution directly influences the accuracy of the numerical results. A smaller grid size generally reduces fluctuations in the simulated data; however, it also increases computational demands and extends simulation time. Conversely, a larger grid size increases numerical error, thereby compromising simulation accuracy. Following the grid independence experiments conducted by McGrattan et al. [25], the characteristic fire diameter D^* is adopted as the principal parameter for evaluating grid resolution. The ratio of the characteristic fire diameter D^* to the grid cell size δx is recommended to fall within the range of 4–16 to ensure accurate computation of fluid viscous stresses in fire simulations. The characteristic fire diameter is calculated using Eq. (1):

$$D^* = \left(\frac{Q}{\rho_0 c_p T_0 g^{\frac{1}{2}}}\right)^{\frac{2}{5}} \quad (1)$$

where, D^* is the heat release rate of the fire source (kW), ρ_0 is the ambient air density (kg/m³), c_p is the specific heat capacity of air (kJ/(kg·K)), T_0 is the ambient temperature (K), and g is the gravitational acceleration (m/s²).

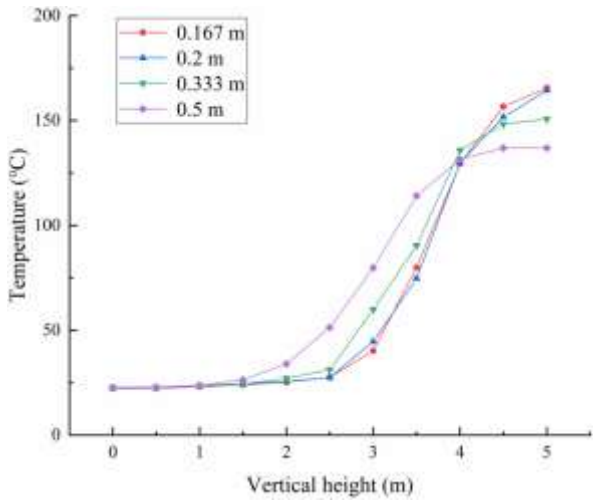

Figure 2. Vertical temperature distribution at a position 8 m from Fire Source A

Using the 5 MW dual fire source scenario as an example, the range of permissible grid sizes was determined to be between 0.15 m and 0.599 m based on the characteristic fire diameter equation and the recommended ratio range. To select an optimal grid resolution, four candidate grid sizes—0.167 m, 0.2 m, 0.333 m, and 0.5 m—were evaluated. Simulations were conducted to examine the vertical temperature distribution at a location 8 m to the left of Fire Source A (Figure 2). The

results indicated that a grid size of 0.5 m produced larger temperature fluctuations, leading to greater numerical error. In contrast, a grid size of 0.333 m yielded stable temperature profiles with acceptable accuracy. Consequently, a grid size of 0.333 m was selected for the final simulations, resulting in approximately 160,000 computational cells for the entire tunnel model.

3. SMOKE CONTROL PERFORMANCE ANALYSIS OF THE SUPPLY-EXHAUST AIR CURTAIN

3.1 Smoke control of the air curtain

The smoke control function of the supply-exhaust air curtain is achieved through the combined action of the bottom-mounted supply curtain and the high-speed exhaust curtain. The supply curtain discharges a uniform upward airflow along the z-axis through its outlet, forming an effective barrier to block smoke propagation, while simultaneously directing toxic and high-temperature smoke toward the exhaust inlet to facilitate efficient removal by the exhaust curtain. Excessive supply velocity can prevent smoke from being effectively drawn into the exhaust inlet and exhausted from the tunnel. Therefore, the supply velocity was fixed at a constant value of 2 m/s. The present analysis focuses on the influence of different dual fire source heat release rates and varying exhaust velocities on smoke control performance, based on numerical simulation results. The smoke propagation patterns are illustrated in Figure 3.

Figure 3. Smoke propagation in a tunnel fire scenario

From Figure 3, it can be observed that when the dual fire source heat release rate is 5 MW and the supply-exhaust air curtain is not in operation, smoke propagates to the tunnel exit within 34 s as the fire develops. When the air curtain system is installed with an exhaust velocity of 1 m/s, the low exhaust rate allows only a limited portion of the smoke to be confined between the two curtains, while most of the hot smoke rapidly penetrates the curtain's working zone and reaches the tunnel exit, resulting in ineffective smoke containment. When the exhaust velocity is increased to 3 m/s, smoke propagation is effectively controlled, and under the action of the air curtain's exhaust capability, no smoke accumulation is observed at the bottom of the unprotected zone, which is favorable for safe evacuation and for fire suppression operations. At an exhaust velocity of 14 m/s, smoke is still effectively contained; however, excessive exhaust induces an entrainment effect, generating a negative pressure region. To balance the pressure difference, external cold air enters through the tunnel portals and fresh air inlets, which hinders the removal of hot smoke. Consequently, smoke descends and accumulates at the bottom of the unprotected zone, leading to higher temperatures, reduced visibility, and unfavorable evacuation conditions. Furthermore, this condition increases energy consumption and reduces economic efficiency, indicating that an appropriate velocity is essential to avoid unnecessary waste.

For the 10 MW dual fire source case, an exhaust velocity of 3 m/s fails to provide effective smoke control, resulting in smoke leakage. Increasing the exhaust velocity to 4 m/s improves the situation, with hot smoke being contained within the curtain's working zone by approximately 20 s after steady-state burning is established. In the 20 MW dual fire source case, an exhaust velocity of 4 m/s is also insufficient to control smoke spread. Increasing the exhaust velocity to 8 m/s successfully contains smoke within the designated range, achieving satisfactory smoke prevention and exhaust performance. These results indicate that as the fire source heat release rate increases, the exhaust velocity must be proportionally increased to effectively control smoke spread under higher power fire scenarios. The simulation results confirm that the supply-exhaust air curtain system is capable of effectively containing smoke spread for different dual fire source conditions. Optimal exhaust velocities for different fire source powers were determined, enabling the achievement of the best possible smoke control performance.

3.2 Temperature distribution of the air curtain

As shown in Figure 4, the temperature contour maps illustrate the distribution of temperatures in a 10 MW dual fire source tunnel fire under different exhaust velocities. The temperature fields were analyzed at 200 s after ignition.

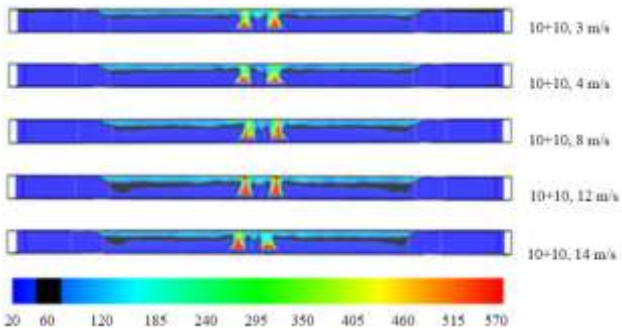

Figure 4. Temperature contour maps of tunnel fires

When the supply velocity was maintained at 2 m/s and the exhaust velocity at 3 m/s, smoke leakage into the protected zone was observed. Increasing the exhaust velocity to 4 m/s significantly improved smoke containment, with most smoke blocked and exhausted from the tunnel, indicating high smoke-blocking efficiency. Consequently, an exhaust velocity of 4 m/s was identified as the threshold condition for evaluating the temperature distribution in the 10 MW dual fire source scenario. For assessment purposes, the short-term human tolerance limit of 60℃ was marked as a black zone in the temperature contour plots. At exhaust velocities of 4 m/s, 8 m/s, 12 m/s, and 14 m/s, smoke was confined within the air curtain region, and the protected zone temperature remained below 30℃—close to the ambient setting of 20℃ and well below the 60℃ tolerance threshold. Furthermore, the temperatures at human evacuation height within the

unprotected zone also remained below 60℃ under all these operating conditions. The differences in temperature distribution among the 4 m/s, 8 m/s, and 12 m/s cases were minimal. The injection of large volumes of cool air by the supply curtain effectively cooled and isolated the hot smoke, while the exhaust inlet simultaneously removed hot gases from the tunnel, demonstrating efficient smoke exhaust performance. Overall, the observed temperature distributions under these conditions satisfied the thermal requirements for safe evacuation.

3.3 Vertical temperature comparison between protected and unprotected zones

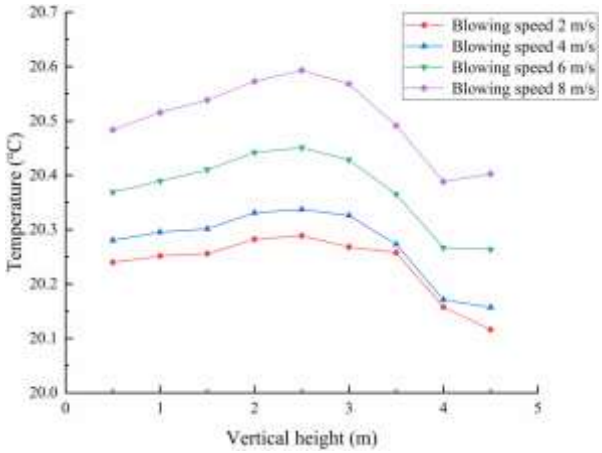

Figure 5. Vertical temperature distribution 5 m from the curtain on the protected side

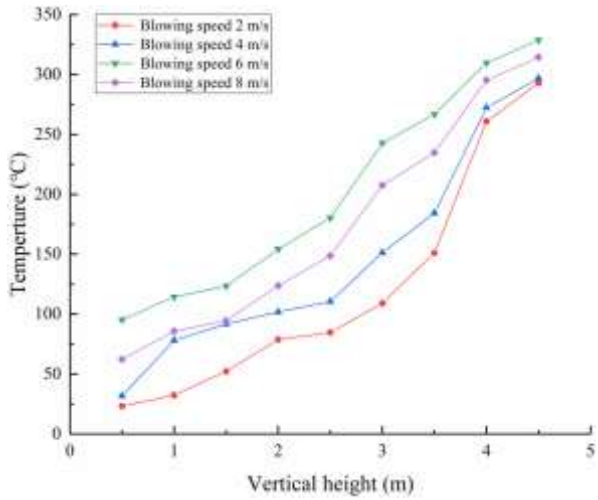

Figure 6. Vertical temperature distribution 5 m from the curtain on the unprotected side

The vertical temperature distribution on both sides of the air curtain in the non-fire source section of the tunnel was analyzed under different supply velocities. Figures 5 and 6 present the vertical temperature profiles measured 5 m from the air curtain on the protected side (outside the curtain) and the unprotected side (inside the curtain), respectively. The results indicate that, under identical conditions of a dual fire source with a heat release rate of 20 MW and an exhaust velocity of 8 m/s, no smoke leakage occurred on the protected side as the supply air velocity increased. In this zone, the vertical temperature distribution from 0.5 m above the tunnel floor to 4.5 m below the ceiling remained approximately 20℃ for all tested supply velocities. By contrast, the unprotected side exhibited a vertical temperature profile characteristic of normal smoke temperature distribution.

On the unprotected side, smoke stratification was observed, with vertical temperature decreasing toward the tunnel floor. At a supply velocity of 2 m/s, the temperature at the human eye level (1.8 m) was approximately 60℃, which meets the short-term safety threshold for evacuation. However, at a supply velocity of 6 m/s, the vertical temperature reached 95℃ at a height of 0.5 m, exceeding the human tolerance limit, and peaked at 328℃ at 4.5 m. These results demonstrate that an excessively high supply velocity does not necessarily improve smoke exhaust efficiency; rather, it can hinder smoke removal, causing accumulation within the tunnel. Based on the present findings, a supply velocity of 2 m/s is considered an appropriate operational parameter for the supply-exhaust air curtain system under the tested conditions.

4. SMOKE EXHAUST PERFORMANCE ANALYSIS OF THE SUPPLY-EXHAUST AIR CURTAIN

4.1 Ceiling temperature variation under different tunnel conditions

When a highway tunnel fire is triggered by incidents such as tire ignition, vehicle collision, or the explosion of flammable materials, the combustion-generated high-temperature smoke forms a buoyant plume that rises freely to the tunnel ceiling. The smoke then spreads horizontally along the ceiling toward both tunnel portals. The longitudinal spread of smoke represents the longest phase in the development of a tunnel fire. The evolution of a fire is typically divided into three stages: the growth stage, the fully developed stage, and the decay stage. During the fully developed stage of a dual fire source scenario, the combustion process is stable, and the ceiling temperature inside the highway tunnel reaches its peak value. A previous study by Gao et al. [26] has demonstrated that thermal interaction between dual fire sources generates a heat feedback effect, in which the entrainment of air between the sources accelerates the combustion rate. This enhanced combustion leads to more rapid smoke accumulation, causing the longitudinal spread of smoke to occur at a higher velocity compared with single fire source scenarios.

Due to the symmetrical distribution of fire-induced smoke with respect to the fire sources, the ceiling temperature data from only the left or right side of the tunnel can be used for analysis. Figures 7 and 8 present, respectively, the variations in ceiling temperature for different dual fire source heat release rates and the ceiling temperature distributions for a 20 MW dual fire source under varying exhaust velocities. As shown in Figure 7, the highest ceiling temperature occurs at the midpoint between the two fire sources, with the peak temperature for the 20 MW dual fire source reaching approximately 1100℃. As the smoke propagates toward the tunnel exits, continuous heat exchange and thermal radiation between the smoke, the surrounding tunnel walls, and the ambient air cause a progressive temperature decrease. Beyond a distance of 20 m from the fire source, the rate of ceiling temperature reduction becomes gradual. In the air curtain zone, a pronounced ceiling temperature difference is observed compared with the region near the fire source. In tunnels equipped with a supply-exhaust air curtain system, a small fraction of smoke may fail to be discharged in time, resulting

in accumulation within the tunnel and a slight increase in temperature. Consequently, the ceiling temperature in such tunnels is marginally higher than that in tunnels without an air curtain; however, the spread of smoke is effectively curtailed, maintaining the ceiling temperature in the protected zone at approximately 20℃. With increasing fire source power, the ceiling temperature correspondingly rises. The maximum temperature difference between 5 MW and 20 MW dual fire sources reaches approximately 800℃. Higher fire source power results in more intense combustion and significantly elevated smoke temperatures. As indicated in Figure 8, variations in ceiling temperature under different exhaust velocities are relatively minor. An increase in exhaust velocity leads to a ceiling temperature rise of less than 10℃, which is counterproductive for reducing the ceiling temperature.

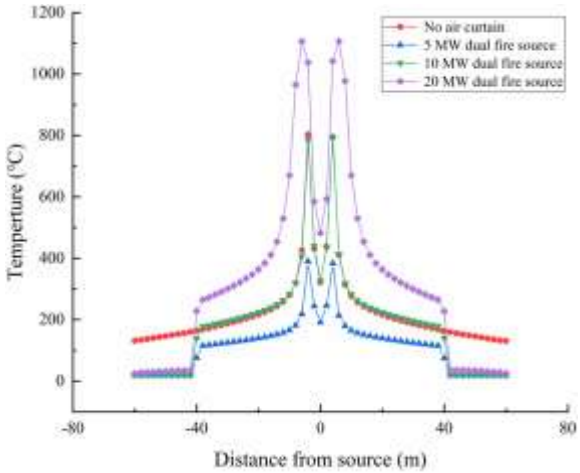

Figure 7. Ceiling temperature for different dual fire source heat release rates

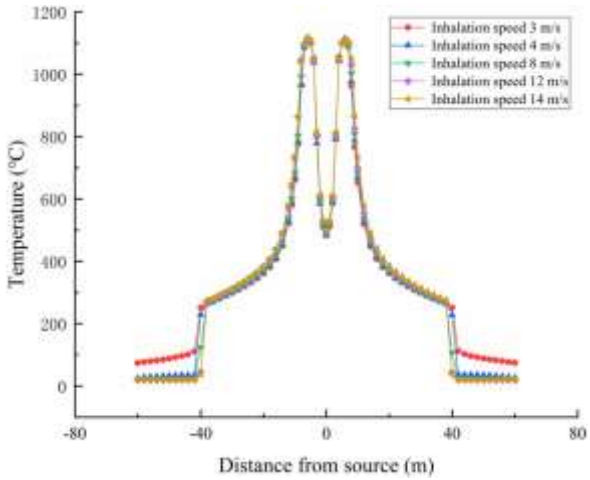

Figure 8. Ceiling temperature for a dual fire source of 20 MW at different exhaust velocities

4.2 Analysis of temperature, CO concentration, and visibility at human characteristic height

4.2.1 Temperature variation at human height under different operating conditions

Figures 9, 10, and 11 present the temperature distributions at a height of 1.8 m above the tunnel floor—the typical height of the human breathing zone—under varying exhaust velocities for dual fire sources of 5 MW, 10 MW, and 20 MW, respectively.

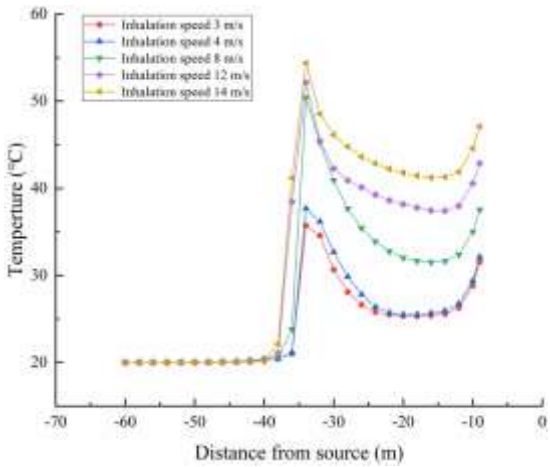

Figure 9. Temperature distribution at human height under different exhaust velocities for the dual fire sources with a heat release rate of 5 MW

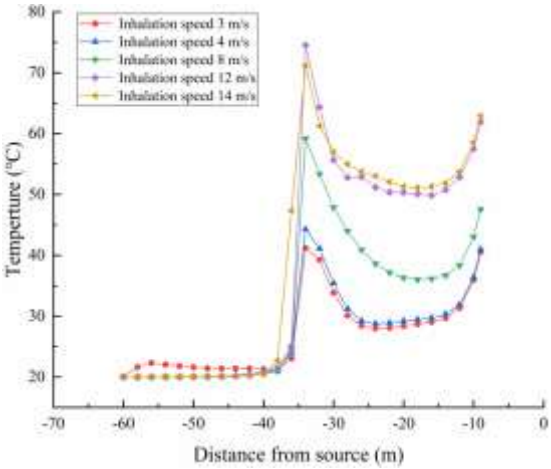

Figure 10. Temperature distribution at human height under different exhaust velocities for the dual fire sources with a heat release rate of 10 MW

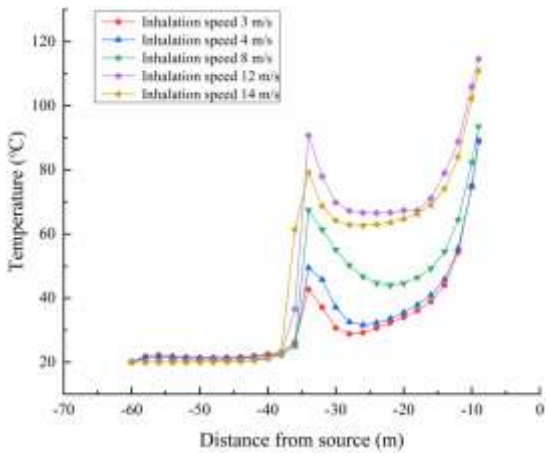

Figure 11. Temperature distribution at human height under different exhaust velocities for the dual fire sources with a heat release rate of 20 MW

Owing to the perfectly symmetrical tunnel model adopted in the simulation, with dual fire sources positioned at the center, only measurement points on the left side of the tunnel were selected for data analysis. The temperature values were derived from the average readings at measurement points

spaced at 2 m intervals over the 360 s duration of the tunnel fire scenario.

Analysis of the data presented in the figures indicates that, with increasing exhaust velocity, the temperature at a height of 1.8 m within the smoke control zone of the supply-exhaust air curtain generally increases. Under higher exhaust velocities, the temperature at human height was found to be higher than that observed under lower velocities. In typical fire scenarios, hot smoke accumulates near the tunnel ceiling to form a stable hot smoke layer, while cooler air descends, creating a vertical temperature gradient. This stratification is beneficial for separating the high-temperature smoke from the evacuation zone. However, when the exhaust velocity becomes excessive, the high-speed exhaust curtain generates intense airflow disturbances at the exhaust inlet. This turbulence entrains hot smoke from the ceiling downward, mixing it into the evacuation zone and thereby elevating the temperature at human height. Additionally, the high-speed exhaust curtain may induce a negative pressure effect, drawing in more fresh air that supplies oxygen to the fire source, thereby intensifying combustion and increasing heat release. This additional heat is then transported by airflow to the human-height region. It was also observed that the temperature on the smoke control side of the air curtain was relatively higher due to the intense mixing between the supply-exhaust air curtain and the high-temperature smoke in the contact region.

While the injection of cold air from the air curtain can dilute the smoke, the mixing process promotes heat exchange between the cold air and the hot smoke, locally increasing the temperature. Within the personnel protection zone on the left side of the air curtain, the overall temperature remained stable at approximately 20℃, while in the smoke control zone on the right side, the temperature at human height generally remained below 60℃. Exceptions were noted only for certain measurement points in the dual-fire-source scenario with a total heat release rate of 20 MW, where temperatures slightly exceeded 60℃. Comparing the temperatures at human height for different dual fire sources, it was found that the 5 MW case consistently remained below 60℃, whereas both overall and local temperatures increased with higher fire source power. This trend is attributed to the fact that greater fire source power results in more heat being released per unit time, producing a larger volume of higher-temperature smoke. Larger fire sources generate fire plumes that accelerate smoke spread, and during this transport, the surrounding air is progressively heated through thermal conduction and thermal radiation, causing a general rise in temperature.

4.2.2 Variation in visibility at human height under different operating conditions

As shown in Figures 12, 13, and 14, the variations in visibility at a height of 1.8 m above the floor were examined for dual fire sources with heat release rates of 5 MW, 10 MW, and 20 MW, respectively, under different exhaust velocities.

For the 5 MW and 10 MW dual fire source scenarios, visibility within the vicinity of the fire sources was observed to be below 10 m, whereas in all other areas visibility exceeded 10 m. Within the air curtain protection zone, visibility values reached approximately 30 m.

With increasing exhaust velocity, high-speed exhaust airflow was found to potentially disrupt the internal tunnel airflow distribution, hindering the effective removal of smoke. This disruption can cause smoke to accumulate within the tunnel, increasing smoke concentration and thereby reducing visibility. Moreover, high-velocity jets may drive smoke toward the tunnel ceiling or sidewalls, resulting in a more uneven smoke distribution and consequently lowering visibility in unprotected regions.

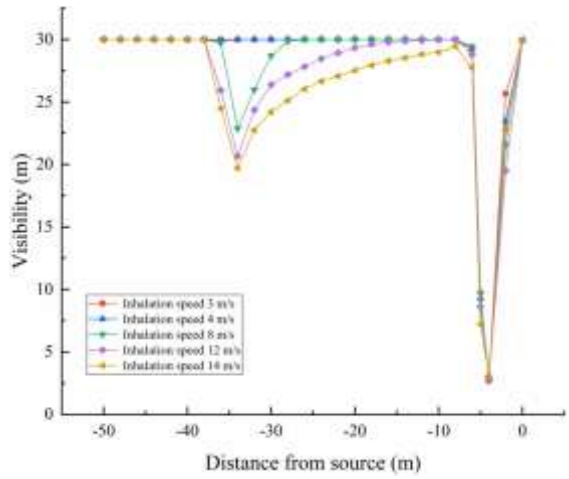

Figure 12. Variation in visibility under different exhaust velocities for a dual fire source of 5 MW

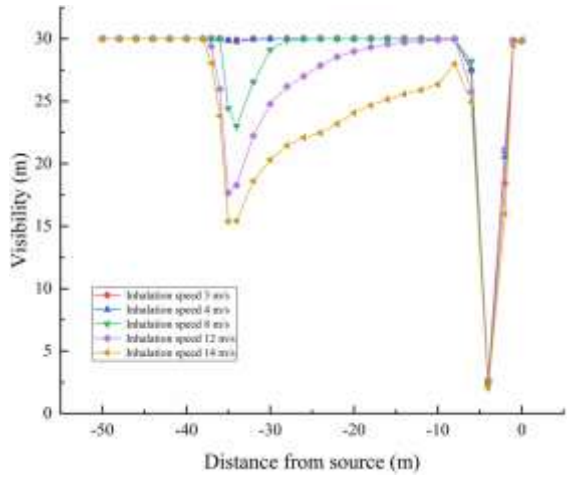

Figure 13. Variation in visibility under different exhaust velocities for a dual fire source of 10 MW

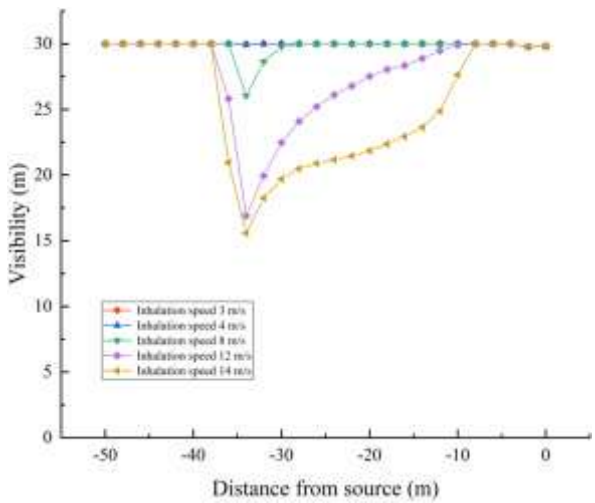

Figure 14. Variation in visibility under different exhaust velocities for a dual fire source of 20 MW

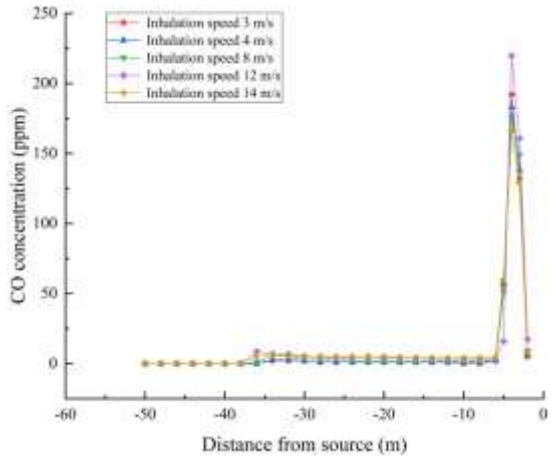

Figure 15. Variation in CO concentration under different exhaust velocities for dual fire sources with a heat release rate of 5 MW

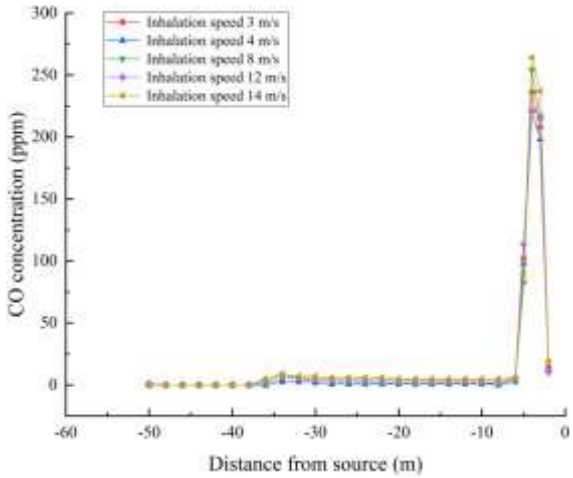

Figure 16. Variation in CO concentration under different exhaust velocities for dual fire sources with a heat release rate of 10 MW

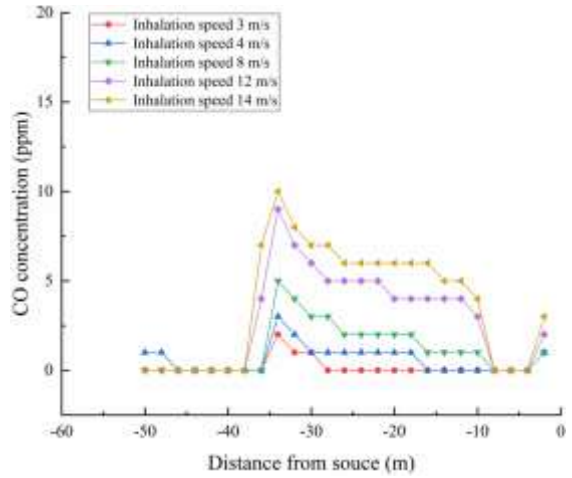

Figure 17. Variation in CO concentration under different exhaust velocities for dual fire sources with a heat release rate of 20 MW

4.2.3 Variation of CO concentration at human height under different operating conditions

As shown in Figures 15, 16, and 17, the variations in CO concentration (ppm) at a height of 1.8 m above the ground were compared for dual fire sources of 5 MW, 10 MW, and 20 MW, respectively, under different exhaust velocities. The data indicate that the CO concentration increases with rising exhaust velocity; however, the increments remain within a controllable range. According to the relevant safety standards for CO exposure, a threshold concentration of 50 ppm was adopted as the criterion for the safe evacuation of personnel. The results show that the CO concentration at human height generally stabilizes at approximately 10 ppm, which is far below the threshold for human health hazards and thus meets the conditions required for personnel evacuation. Elevated CO concentrations were observed in the vicinity of the fire sources, with peak values reaching 264 ppm and 237 ppm. This increase is attributed to insufficient oxygen supply near the fire sources during highway tunnel fires, particularly in the early stages of fire development or under poor ventilation conditions. Oxygen deficiency leads to incomplete combustion, resulting in substantial CO generation. Furthermore, restricted airflow within the tunnel causes dense smoke to accumulate near the fire sources, leading to a rapid rise in CO concentration.

4.3 Analysis of CO mass flow rate exhaust efficiency

The exhaust efficiency was evaluated as the percentage ratio of the CO mass flow rate at the exhaust curtain to the CO mass flow rate generated by the dual fire sources per unit time in a highway tunnel. This parameter was adopted as an indicator to assess the smoke exhaust performance of a supply-exhaust air curtain under dual fire-source conditions.

Heptane was employed as the fuel for the dual fire sources, with a calorific value of 45,534.34 kJ/kg. The incomplete combustion of heptane follows the reaction equation:

$$C_7H_{16} + 10.862O_2 \rightarrow 6.855CO_2 + 7.933H_2O + 0.0214CO + 0.1376Soot \quad (2)$$

Based on this equation, the CO mass flow rates generated per unit time by fire sources of 5 MW, 10 MW, and 20 MW were calculated to be 0.6579 g/s, 1.3158 g/s, and 2.6316 g/s, respectively. The CO mass flow rate at the exhaust inlet was determined by multiplying the average measured CO mass flow rate at the exhaust inlet by its cross-sectional area. The exhaust efficiency of the supply-exhaust air curtain was then obtained as shown in Table 2, which presents the efficiency values under various combinations of dual fire-source intensities, exhaust velocities, and supply velocities.

Table 2 presents the smoke exhaust efficiency under various tunnel fire scenarios. The data indicate that smoke exhaust efficiency does not invariably increase with higher exhaust velocities; on the contrary, a decreasing trend is observed in most cases. Excessive exhaust velocities were found to disrupt smoke stratification. When the exhaust velocity was increased from 4 m/s to 14 m/s, a general decline in extraction efficiency occurred, as exemplified by the 5 MW + 5 MW dual fire source scenario, where efficiency decreased from 57.2% to 39.0%. This suggests that overly strong exhaust flows can interfere with the buoyancy-driven upward movement of smoke, leading to excessive dilution or dispersion into non-target zones. For the 20 MW dual fire source, smoke exhaust efficiencies of 93% and 80% were achieved at supply velocities of 4 m/s and 6 m/s, respectively. However, excessive supply velocities may induce airflow turbulence, reducing temperature and visibility at occupant height, thereby compromising evacuation and rescue conditions.

Table 2. Smoke extraction efficiency under different tunnel fire scenarios

Dual Fire Source Heat Release Rate	Supply Velocity	Exhaust Velocity	Smoke Extraction Efficiency
5 MW + 5 MW	2 m/s	4 m/s	57.2%
5 MW + 5 MW	2 m/s	8 m/s	53.5%
5 MW + 5 MW	2 m/s	12 m/s	43.8%
5 MW + 5 MW	2 m/s	14 m/s	39%
10 MW + 10 MW	2 m/s	4 m/s	76%
10 MW + 10 MW	2 m/s	8 m/s	68.1%
10 MW + 10 MW	2 m/s	12 m/s	51.1%
10 MW + 10 MW	2 m/s	14 m/s	51.1%
20 MW + 20 MW	2 m/s	8 m/s	62%
20 MW + 20 MW	2 m/s	12 m/s	76.6%
20 MW + 20 MW	2 m/s	14 m/s	73%
20 MW + 20 MW	4 m/s	8 m/s	93%
20 MW + 20 MW	6 m/s	8 m/s	80%

The influence of fire source power on smoke exhaust efficiency is evident. For the 5 MW dual fire source, efficiencies were relatively low (<60%), indicating limited smoke control capability of the supply-exhaust air curtain system for small-scale fires. This may be attributed to the weaker thermal buoyancy generated by smaller fire sources, resulting in insufficient upward momentum of smoke and reduced guidance effectiveness by the air curtain. Under such conditions, lower supply velocities (2 m/s) and moderate exhaust velocities (4–8 m/s) are recommended to prevent efficiency loss caused by excessive airflow. For the 10 MW dual fire source, smoke exhaust efficiency was moderately improved (51.1%–76%), although still notably affected by exhaust velocity. In contrast, the 20 MW dual fire source exhibited significantly higher efficiencies (62%–93%), with the highest efficiency of 93% achieved at a supply velocity of 4 m/s and an exhaust velocity of 8 m/s. These results indicate that the air curtain system is more effective for large-scale fires, as the stronger thermal buoyancy facilitates the transport of hot smoke by the induced airflow.

5. CONCLUSION

A tunnel fire model incorporating a supply-exhaust air curtain system under dual fire source scenarios was established using FDS. Multiple simulation conditions and data monitoring points were configured to examine the effects of varying dual fire source heat release rates and air curtain velocities on smoke control, vertical temperature distribution, temperature at occupant height, visibility, CO concentration distribution, and smoke exhaust efficiency. The main conclusions are as follows:

(a) Optimal exhaust velocity parameters for the supply-exhaust air curtain were determined for different dual fire source heat release rates. For a total heat release rate of 5 MW, an exhaust velocity of 3 m/s effectively controlled high-temperature smoke. For 10 MW, an exhaust velocity of 4 m/s achieved effective control, while for 20 MW, an exhaust velocity of 8 m/s was required to maintain effective smoke suppression.

(b) In the case of a 10 MW dual fire source scenario, variations in exhaust velocities of 4 m/s, 8 m/s, and 12 m/s produced negligible differences in temperature distribution. The injection of a large volume of cool air into the tunnel by the air curtain demonstrated a strong cooling and isolating effect on hot smoke. Analysis of the vertical temperature variation on both sides of the air curtain indicated that excessively high supply velocities could disrupt normal smoke exhaust; therefore, a supply velocity of 2 m/s was identified as optimal.

(c) Under various fire scenarios, larger dual fire source heat release rates led to higher ceiling temperatures, peaking consistently at the midpoint between the sources. Smoke temperature decreased as it spread, while significant ceiling temperature differences persisted between the air curtain zone and fire source areas. In unprotected zones, occupant-height temperatures stayed below the 60℃ tolerance threshold. Visibility dropped below 10 m only near 5 MW and 10 MW fire sources, remaining above 10 m elsewhere, with the air curtain zone maintaining around 30 m. CO levels stayed below 10 ppm, except near fire sources, ensuring safe evacuation in most areas.

(d) Smoke exhaust efficiency did not consistently increase with higher exhaust velocities and, in most cases, exhibited a declining trend. The supply-exhaust air curtain system demonstrated strong smoke control capability for large-scale dual fire source fires. Although increasing the supply velocity significantly enhanced smoke exhaust efficiency, it also caused multiple parameters at occupant height to exceed safety thresholds, thereby compromising evacuation conditions.

ACKNOWLEDGMENT

This paper was supported by the Research and Practice Project on Reforming Research-Based Teaching in Undergraduate Colleges and Universities in Henan Province (Grant No.: 2022SYJXLX045).

REFERENCES

[1] Chen Z Y, Liu Z X, Huang L Q. Research on the effect of ceiling centralized smoke exhaust system with air curtains on heat confinement and plug-holing phenomenon in tunnel fires. Process Safety and Environmental Protection, 2023, 169: 646-659. https://doi.org/10.1016/j.psep.2022.11.054

[2] Yang, J., Ye, J. (2024). Study on temperature field beneath tunnel ceiling induced by transverse symmetrical double fires. International Journal of Thermal Sciences, 204: 109239. https://doi.org/10.1016/j.ijthermalsci.2024.109239

[3] Oka, Y., Imazeki, O. (2015). Temperature distribution within a ceiling jet propagating in an inclined flat-ceilinged tunnel with natural ventilation. Fire Safety

Journal, 71; 20-33. https://doi.org/10.1016/j.firesaf.2014.11.002
[4] Wang, Q., Wang, S., Liu, H., Shen, J., Shang, F., Shi, C., Tang, F. (2020). Characterization of ceiling smoke temperature profile and maximum temperature rise induced by double fires in a natural ventilation tunnel. Tunnelling and Underground Space Technology, 96: 103233. https://doi.org/10.1016/j.tust.2019.103233
[5] Jia, Y., Fan, X., Zhao, X., Deng, Y., Zhu, X., Zhao, W. (2021). Study on the longitudinal ceiling temperature distribution induced by double pool fires in a tunnel. International Journal of Thermal Sciences, 168: 107059. https://doi.org/10.1016/j.ijthermalsci.2021.107059
[6] Yan, G.F, Wang, M.N., Yu, L., Tian, Y., Guo, X.H. (2019). Study of smoke movement characteristics in tunnel fires in high-altitude areas. Fire and Materials, 44(1): 65-75. https://doi.org/10.1002/fam.2770
[7] Krajewski, G., Węgrzyński, W. (2015). Air curtain as a barrier for smoke in case of fire: Numerical modelling. Bulletin of the Polish Academy of Sciences: Technical Sciences, 63(1): 145-153. https://doi.org/10.1515/bpasts-2015-0016
[8] Jung, U.H., Kim, S., Yang, S.H., Kim, J.H., Choi, Y.S. (2016). Numerical study of air curtain systems for blocking smoke in tunnel fires. Journal of Mechanical Science and Technology, 30(11): 4961-4969. https://doi.org/10.1007/s12206-016-1016-6
[9] Ji, J., Lu, W., Li, F., Cui, X. (2022). Experimental and numerical simulation on smoke control effect and key parameters of Push-pull air curtain in tunnel fire. Tunnelling and Underground Space Technology, 121: 104323. https://doi.org/10.1016/j.tust.2021.104323
[10] Gao, D., Li, T., Mei, X., Chen, Z., et al. (2020). Effectiveness of smoke confinement of air curtain in tunnel fire. Fire Technology, 56(5): 2283-2314. https://doi.org/10.1007/s10694-020-00977-z
[11] Moureh, J., Yataghene, M. (2016). Numerical and experimental investigations on jet characteristics and airflow patterns related to an air curtain subjected to external lateral flow. International Journal of Refrigeration, 67: 355-372. https://doi.org/10.1016/j.ijrefrig.2016.03.002
[12] Halawa, T. (2022). Enhancement of smoke extraction in tunnels in the case of fire by using L-shape curtain near smoke extraction vents. Case Studies in Thermal Engineering, 33: 101969. https://doi.org/10.1016/j.csite.2022.101969
[13] Zhang, T., Han, R. (2023). Numerical study on the influence of subway platform air curtains on smoke diffusion. Case Studies in Thermal Engineering, 50: 103439. https://doi.org/10.1016/j.csite.2023.103439
[14] Lu, X., Weng, M., Liu, F., Yu, J. (2024). Study on smoke sealing effectiveness of the air curtain in exit bifurcated tunnel fires. Case Studies in Thermal Engineering, 63: 105380. https://doi.org/10.1016/j.csite.2024.105380
[15] Yu, L.X., Liu, F., Beji, T., Weng, M.C., Merci, B. (2018). Experimental study of the effectiveness of air curtains of variable width and injection angle to block fire-induced smoke in a tunnel configuration. International Journal of Thermal Sciences, 134: 13-26. https://doi.org/10.1016/j.ijthermalsci.2018.07.044
[16] Zhang, L., Yan, Z., Li, Z., Wang, X., Han, X., Jiang, J. (2018). Study on the effect of the jet speed of air curtain on smoke control in tunnel. Procedia Engineering, 211: 1026-1033. https://doi.org/10.1016/j.proeng.2017.12.106
[17] He, K., Shi, L., Zhang, S., Cong, W., Yang, H., Cheng, X. (2023). Experimental study on temperature attenuation of smoke flow driven by dual fire sources in a tunnel. Tunnelling and Underground Space Technology, 134: 105004. https://doi.org/10.1016/j.tust.2023.105004
[18] Guo, C., Pan, Y., Wang, K., Zhou, X., Yan, Z. (2024). Full-scale experimental study on combustion characteristics and smoke temperature of double-source fires in different tunnels. Fire Safety Journal, 146: 104177. https://doi.org/10.1016/j.firesaf.2024.104177
[19] Wan, H., Xiao, Y., Wei, S., Zhang, Y., Oka, Y. (2023). Experimental study on multiple fire hazards in a naturally ventilated tunnel: assessment of the flame interaction and extension of two unequal fires. International Journal of Thermal Sciences, 187: 108209. https://doi.org/10.1016/j.ijthermalsci.2023.108209
[20] Li, J., Liu, W., Li, Y.F., Chow, W.K., Chow, C.L., Cheng, C.H. (2022). Scale modelling experiments on the effect of longitudinal ventilation on fire spread and fire properties in tunnel. Tunnelling and Underground Space Technology, 130: 104725. https://doi.org/10.1016/j.tust.2022.104725
[21] Zhao, S., Du, K., Yao, Y., Wang, F., Weng, M., Xu, L., Lei, W. (2023). Influence of sidewall restriction on flame characteristics of double fires in a channel. Tunnelling and Underground Space Technology, 140: 105297. https://doi.org/10.1016/j.tust.2023.105297
[22] National Fire Protection Association. (2011). NFPA 502, Standard for road tunnels, bridges, and other limited access highways. NFPA.
[23] Chen, Z., Liu, Z., Li, X., Linqi, H., Niu, G. (2022). Numerical study of the effect of air curtains on smoke blocking and leakage heat flux in tunnel fires. Case Studies in Thermal Engineering, 35: 102164. https://doi.org/10.1016/j.csite.2022.102164
[24] Caliendo, C., Ciambelli, P., De Guglielmo, M.L., Meo, M. G., Russo, P. (2012). Numerical simulation of different HGV fire scenarios in curved bi-directional road tunnels and safety evaluation. Tunnelling and Underground Space Technology, 31: 33-50. https://doi.org/10.1016/j.tust.2012.04.004
[25] McGrattan, K., Hostikka, S., McDermott, R., Floyd, J., Weinschenk, C., Overholt, K. (2013). Fire Dynamics Simulator User's Guide. NIST Special Publication, Sixth Edition.
[26] Gao, Z., Zhao, P., Wu, Z., Cai, J., Li, L. (2024). Study on the natural smoke exhaust performance of board-coupled vertical shaft in high-altitude tunnel fires. Fire, 7(8): 274. https://doi.org/10.3390/fire7080274